Arch. Metall. Mater. **63** (2018), 3, 1093-1100

DOI: 10.24425/123781

A. TORKIAN*, G. FARAJI*#, M. KARIMPOUR*

MECHANICAL PROPERTIES AND MICROSTRUCTURE OF WE43 Mg ALLOY PROCESSED BY WARM ECAP FOLLOWED BY EXTRUSION

In the present paper, the effects of the subsequent extrusion after multi-pass equal-channel angular pressing (ECAP) process on the mechanical properties and microstructure of WE43 magnesium alloy are investigated. First, second and fourth passes ECAP followed by an extrusion process are applied on WE43 magnesium alloy to refine the microstructure and to improve the mechanical properties for biomedical applications. The results showed that among the ECAPed samples, the highest and lowest strength were obtained in the second and the first pass processed samples, respectively. The four passes processed sample showed the highest elongation to failure with moderate strength. The sample processed via first pass ECAP followed by extrusion exhibits an excellent combination of ductility and strength. The highest strength was obtained in the sample processed via the second pass ECAP followed by extrusion while the highest elongation was achieved in the sample processed via fourth pass ECAP followed by extrusion. Moreover, Vickers micro-indentation tests demonstrate that hardness is enhanced by an increase in the number of ECAP passes. Furthermore, a grain refinement process is presented for ECAP processing of WE43 alloy which shows a good agreement with microstructural investigations.

Keywords: Severe plastic deformation; WE43; Microstructure; Hardness; Mechanical properties

1. Introduction

It is well known that the use of severe plastic deformation (SPD) techniques is one of the most effective ways to refine the grain size and microstructure of polycrystalline metals. Hence, many SPD techniques with various parameters were developed in the last two decades. Diverse studies were also devoted to optimizing the effective parameters [1,2]. High-Pressure Torsion (HPT) [1], Equal Channel Angular Pressing (ECAP) [3-6], Twist Extrusion (TE) [7,8], Cyclic Extrusion Compression (CEC) [9], and Tubular Channel Angular Pressing (TCAP) [10, 11] are among principal SPD processes suitable for deforming bulk metals. A very large plastic strain of about 4-6 or higher is applied to the sample which causes refining the metal structure. This grain refinement can improve some of the mechanical properties such as hardness and strength according to Hall-Petch equation [12]. Among the SPD methods, ECAP is one of the most practical techniques introduced by Segal in 1970s [13]. In this approach, the sample laterally extruded through two equal cross-sectional channels that intersecting with a specific angle normally 90°. Plastic strain is induced into the sample at the intersecting shear region. This procedure can be repeated for more than one time via different routes. Four common routes are *A* in which the sample pressed without any rotation, B_A in which the sample is rotated 90° alternatively, B_c in which the sample is rotated 90° in the same direction and *C* in which the sample is rotated 180° between consequent passes [12]. The combination of ECAP and extrusion may give better properties than the only ECAP. Therefore, various studies have been conducted on different metals and alloys to investigate technique above. Vladimir et al. [14] applied it to commercially pure titanium (CP). Another research was performed to study the mechanical behavior and microstructural evolution of CP Ti by Kang et al. [15].

Magnesium and its alloys due to their relatively low strength are appropriate candidates for SPD processing to enhance their properties [16,17]. Tao et al. [18] conducted a study on ZK60 alloy taking four different conditions into account to compare effects of subsequent extrusion on the microstructure and properties of ZK60 Mg alloy. Their results showed that subsequent extrusion has a significant effect on the microstructure refined by ECAP. Vinogradov et al. [19] improved fatigue behavior of ZK60 Mg alloy. Observations showed that the mechanical properties such as ductility and ultimate strength are enhanced beside fatigue strength. Another research was carried out on AZ31 Mg alloy by Kim et al. [20] to produce high strength micro gears. Grain refinement due to ECAP was achieved while extrusion restored ECAP texture to the state before ECAP which result in hardness improvement. Straska et al. [21] analyzed the thermal stability of ultra-fine grained (UFG) AZ31 Mg alloy. A study was conducted by Miyahara et al. [22] to achieve UFG micro-

* UNIVERSITY OF TEHRAN, SCHOOL OF MECHANICAL ENGINEERING, COLLEGE OF ENGINEERING, TEHRAN, 11155-4563, IRAN

Corresponding author: ghfaraji@ut.ac.ir

structure in AZ61 Mg alloy. It was reported that EX-ECAP is an excellent method to get UFG with a grain size of 0.6-1.3 µm after pressing at 200 and 250°C. Microstructural refinement of the Mg-2Y-1Zn alloy was investigated by Garces et al. [23] to optimize its strength. They reported that extrusion achieved higher strengthening at lower temperatures. Akbaripanah et al. [24] processed AM60 Mg alloy samples up to six passes ECAP at 220°C and obtained grain size reduction from 19.2 µm to 2.3 µm. Their results showed that the yield and ultimate tensile strengths were improved up to two passes. Also, some researchers studied Mg alloys suitable for bioabsorbable biomedical implants. Among them, Minarik et al. [25,26] investigated microstructure and mechanical properties of LAE442 Mg alloy. Among all the biomedical Mg alloy, WE43 is one of the most useful and suitable materials because it is free of any toxic elements such as Al [27].

So far, a few studies were conducted on extrusion of pre-ECAP processed samples. To the best of our knowledge, no studies investigated the extrusion of pre-ECAP processed WE43 magnesium alloy and its effect on the microstructure and mechanical properties. Therefore, the aim of the present study is to examine the effects of subsequent extrusion of pre-ECAP processed WE43 samples on the microstructure and mechanical properties.

2. Experimental procedure

In this paper, WE43 magnesium alloy with the composition shown in Table 1 was used as the experimental material. The rod samples with 10 mm diameter and 70 mm length were cut out by wire electro-discharge machining from extruded bars. ECAP and extrusion dies were manufactured with hot-worked tool steel with 55 HRC hardness. A channel angle of $\varphi = 90°$ and the curvatures angle of $\psi = 20°$ were selected for ECAP die. The extrusion die designed with a 10 mm entrance and 5 mm exit channel (75% reduction). Both ECAP and extrusion processes were accomplished at a pressing speed of 5 mm/min at the temperature of 330°C. The temperature increases by using an electrical heater around the die set to ensure isothermal condition during the process. Before the process, Molybdenum disulfide (MoS_2) was employed to lubricate sample, die and punch surfaces to decrease the friction.

Mechanical properties of the samples were examined by tensile testing done at a strain rate of 10^{-3} 1/s at room temperature. Cylindrical tensile test samples of 3 mm diameter and 10 mm gauge length were prepared from processed and unprocessed specimens.

The schematic of the processes is depicted in Fig. 1. As shown, a sample with a diameter of 10 mm is put in the die channel, and punch starts to move down (Fig. 1a). Then, the punch was removed, and the next sample was put in the die channel (Fig. 1b). Afterward, it presses again, so that WE43 sample completely exits from the die (Fig. 1c). For the next passes, route B_c was used. Then, ECAP processed samples up to four passes were extruded by the extrusion die shown in Fig. 1d.

TABLE 1

Elemental composition of the WE43 magnesium alloy (wt %)

Element	Mg	Y	Nd	Zr	La
Value (wt %)	Bal.	4.12	2.15	0.43	0.26

Equivalent strain in ECAP process is determined by a relationship including the channel angle, φ, and the curvature angle, ψ, as following [28]:

$$\bar{\varepsilon}_{ECAP} = \left(N/\sqrt{3}\right)\left[\begin{array}{l} 2Cot\left\{\left(\varphi/2\right)+\left(\psi/2\right)\right\}+ \\ +\psi\,Cos\,ec\left\{\left(\varphi/2\right)+\left(\psi/2\right)\right\} \end{array}\right] \quad (1)$$

For the extrusion process equivalent strain is achieved by the following formula [29]:

$$\bar{\varepsilon}_{Extrusion} = \ln R \quad (2)$$

Where R is the extrusion ratio equal to A_0/A_s in which A_0 is the initial cross-section of the sample and A_s is the final cross section.

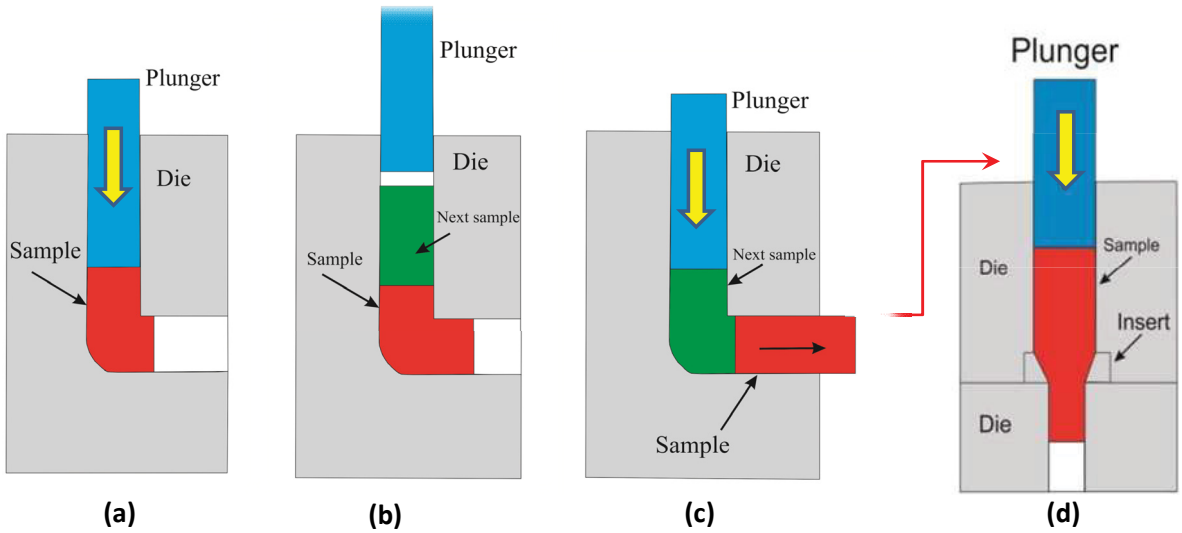

Fig. 1. Schematic of subsequent extrusion followed by ECAP process

TABLE 2

Equivalent strain applied to the samples

Sample	1P-ECAPed	2P-ECAPed	4P-ECAPed	1P + Ex	2P + Ex	4P + Ex
Equivalent plastic strain	1.015	2.03	4.06	2.402	3.4177	5.4491

So, total accumulated plastic strain after combined process could be calculated as follows:

$$\bar{\varepsilon}_{Total} = \bar{\varepsilon}_{ECAP} + \bar{\varepsilon}_{Extrusion} \quad (3)$$

Equivalent plastic strain applied to the samples processed in different conditions was calculated by Eq. (3), and the values were given in Table 2.

ECAPed and extruded specimens were cut out perpendicular to the extrusion direction, polished and etched in a proper solution of 10 ml acetic acid, 70 ml ethanol, 4.2 g picric acid, and 10 ml distilled H_2O to examine the microstructural evolution using optical microscopy (OM). The alloy phases were identified by X-ray diffraction (XRD) with Cu Kα radiation. The composition of phases was examined using energy dispersive X-ray spectrometry (EDS) mode of scanning electron microscopy (SEM). Vickers microhardness measurement was conducted with a load of 100 gr applied for 10 seconds. As shown schematically in Fig. 2, samples for tensile and microhardness tests were prepared.

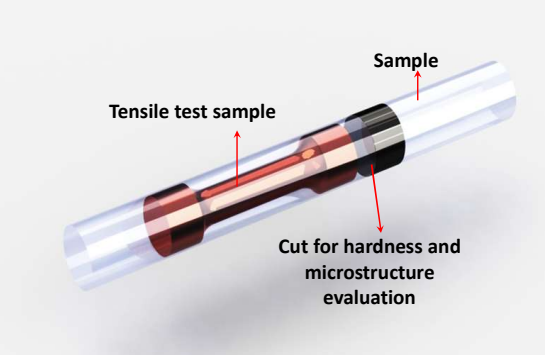

Fig. 2. Schematic demonstration of prepared samples for tensile, microstructure and hardness tests.

3. Results and discussion

Fig. 3 demonstrates the pictures of unprocessed and processed samples via different routes. Due to the circular geometry of the matrix and the formation of burrs, samples were machined between each pass. At the final pass i.e. fourth, small cracks were observed on the sample perimeter. Extruded samples were also shown on the right-hand side of Fig. 3.

3.1. Tensile properties

Stress-strain behaviors of the samples prepared via different processes were indicated in Fig. 4. Fig. 4a illustrates the comparison of stress-strain curves of unprocessed (denoted as

Fig. 3. Unprocessed, ECAPed and extruded samples illustration

"0P"), one pass ECAPed (denoted as "1P") and one pass ECAPed + Extruded samples (denoted as "1P+Ex"). Fig. 4b and 4c show same comparisons for second and fourth ECAP passes, respectively. It can be seen that increase in ECAP passes results in improvement of the material strength. The results showed that among the ECAPed samples, the highest and lowest strengths were obtained in second and the first pass processed sample, respectively. The four passes processed sample showed the highest elongation to failure with moderate strength. However, the trend in combined multi-pass ECAP and Extruded samples are different with ECAP processed specimens. The sample processed via first pass ECAP followed by extrusion exhibits an excellent combination of ductility and strength. The highest strength was obtained in the sample processed via the second pass ECAP followed by extrusion while the highest elongation was achieved in that processed via fourth pass ECAP followed by extrusion. It is important to note that containing some amount of Zr in solid solution that is an effective grain-refining factor in Al-free magnesium alloys also assist sample strengthening [30].

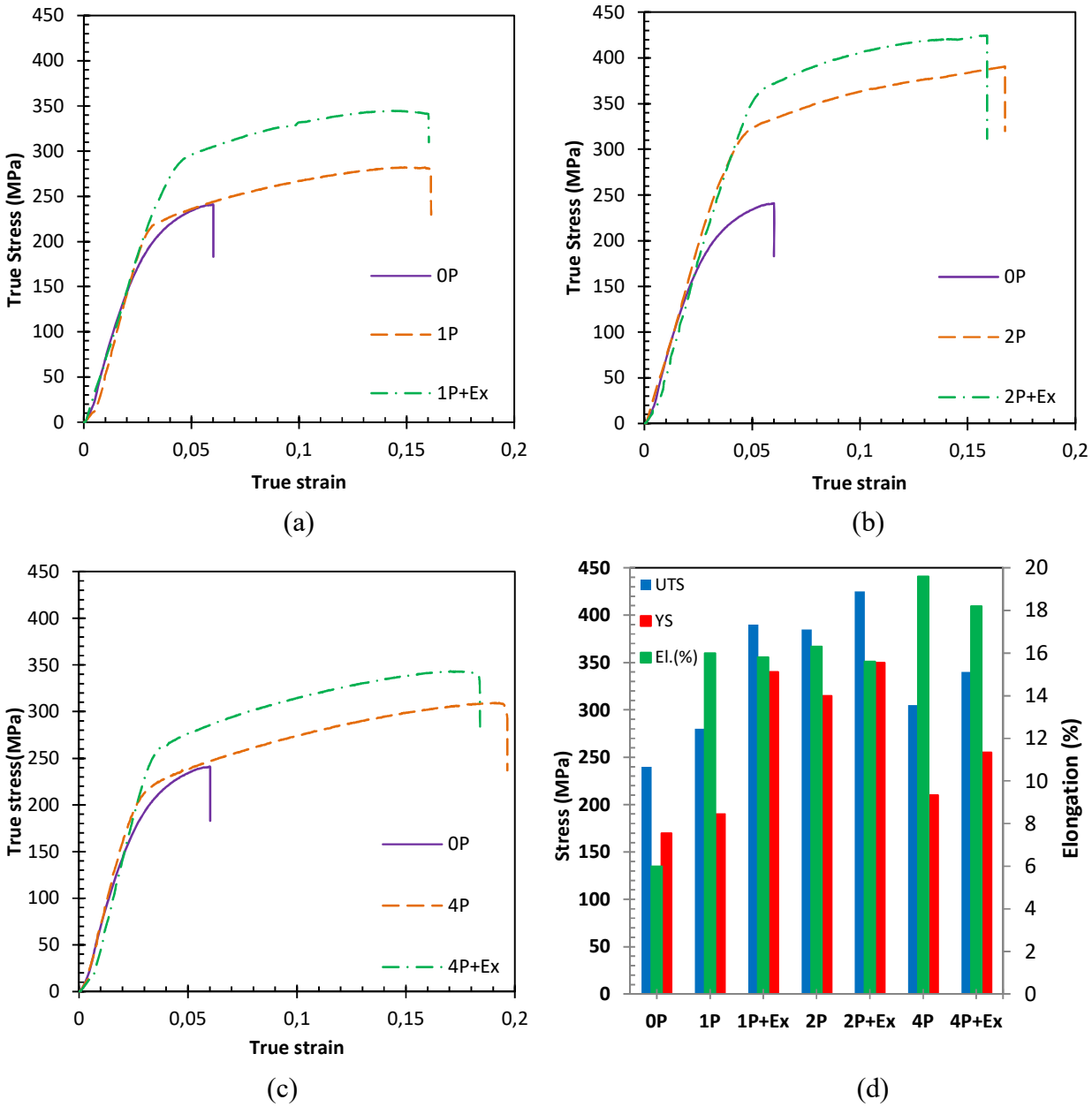

Fig. 4. True stress-strain curves for the ECAPed and ECAPed+extruded WE43 alloy for (a) one (b) two, (c) four passes and (d) YS, UTS and Elongation to the failure of all samples

Furthermore, plastic deformation mechanisms due to dislocation movement and locking can be taken into account as other reasons of mechanical properties enhancements. By increasing the number of passes, recrystallization of new grains occurs. Therefore, new grains pin the grain boundaries and thus, locking them to each other. Also, the yield strength after the fourth pass ECAP decreases in comparison with the second pass. Such reduction in yield strength was seen in Akbaripanah et al. [24] study on AM60 alloy. They explained this characteristic by texture modification that is typical in ECAP process of Mg alloys. Yield strength reduction was also reported by Kim et al. [20] clarified by a change in texture. Also, results demonstrate that extrusion significantly improves the strength which can be justified by an increase in dislocation density due to plastic deformation and total work hardening. Fig. 4d represents the ultimate tensile strength, the yield strength, and elongation of samples before and after ECAP and extrusion processes. It is important to note that ECAP passes improve elongation. As result shows, the elongation of the sample after four ECAP passes is 19.8% which is 230% higher than 6% elongation of the unprocessed sample. It is proven that only basal slip dominates the plastic deformation of Mg alloys at room temperature due to the high critical resolved shear stress (CRSS) of prismatic slip [31]. So, the non-basal slip has a major effect on the Mg alloys ductility.

The ratio of $\frac{CRSS_{prismatic}}{CRSS_{basal}}$ can be affected by grain size, while grain size reduction will result in lowering the mentioned ratio. As a result, prismatic slip can be activated by grain refinement and afterwards enhance the ductility [32]. However, tensile test

results clarify the fact that extrusion process in higher ECAP passes leads to a reduction in material elongation. Extrusion process changes equiaxed grains formed after ECAP to elongated grains. Moreover, the tensile direction is parallel to these elongated grains. As a result, elongation is reduced due to a decrease in grain boundary density.

3.2. Microstructure

The as-received microstructure of WE43 alloy is shown in Fig. 5. As it can be seen, as-cast sample structure consists of coarse equiaxed grains with ~135 μm in size. The typical microstructure of the alloy is a α-Mg matrix with some dispersed $Mg_{41}Nd_5$ phases through the grains and grain boundaries [33]. Fig. 5 also shows the microstructure of WE43 alloy after multi-pass ECAP and multi-pass ECAP+Extrusion processes. As shown, by increasing deformation passes, the volume fraction of recrystallized grains is increased, and the average grain size

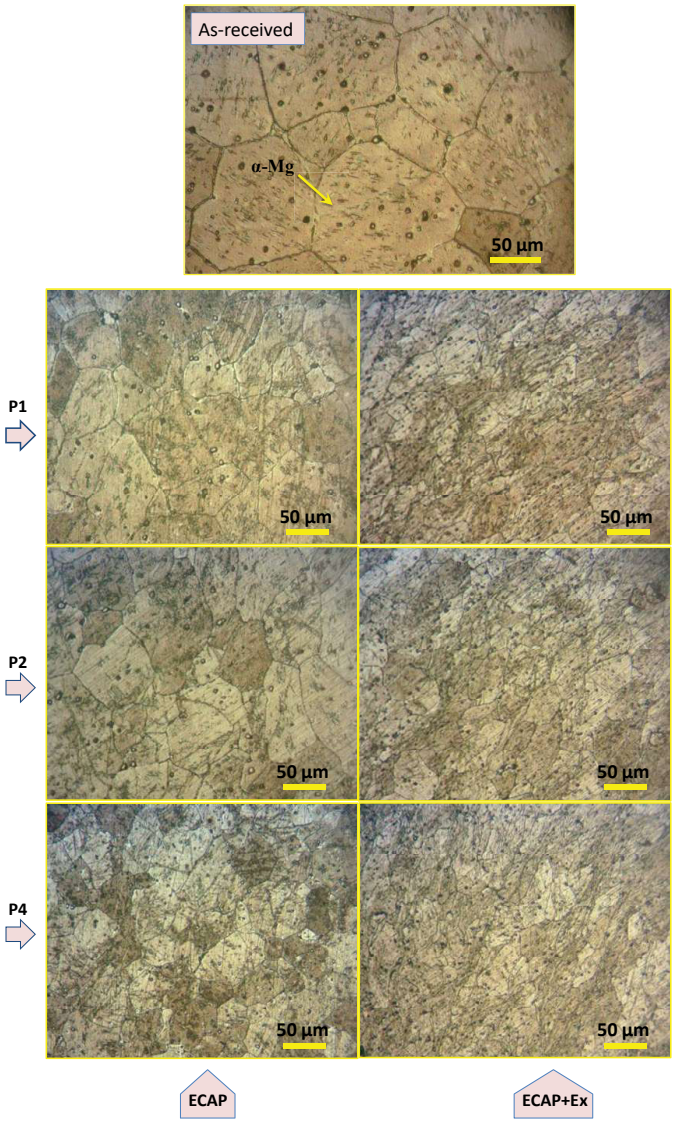

Fig. 5. The microstructure of WE43 before and after ECAP through different passes and ECAP+Extrusion processes

is reduced. Furthermore, the alloy contains some rare elements (RE) such as Y which is larger than Mg [34]. REs inhibit the movement of grain boundaries that are well known as Zener pinning effect. Such alteration in grain shapes is demonstrated in right-hand side images of Fig. 5. Also, new grains are nucleated near the original grain boundaries that can be associated with the strain-induced boundary migration (SIBM) [35]. After the first pass of ECAP process, grain refinement, and better distribution of $Mg_{41}Nd_5$ phase is achieved as shown in Fig. 6. Fig. 7 schematically illustrates grain refining process in multi-pass ECAP process. Fig. 7a shows the unprocessed sample with large equiaxed α-Mg grains and dispersed $Mg_{41}Nd_5$ phase. After the first pass of ECAP, fine new grains with some new $Mg_{41}Nd_5$ phases nucleate along the grain boundaries (Fig. 7b). As shown in Fig. 7c, by performing the second pass of ECAP, the structure becomes more homogenous, the fraction of new grains increases and some coarse grains gradually dissipate. Eventually, at the end of the fourth pass, a structure with fine homogeneous grains develops (Fig. 7d). As shown, large $Mg_{41}Nd_5$ phase within the grain interiors is seen in the unprocessed microstructure. After the first pass of ECAP new small $Mg_{41}Nd_5$ phase and new dynamically recrystallized grains are formed along the initial grain boundaries. Further straining leads to the forming of more new finer recrystallized grains. In this stage, the area fraction of the un-recrystallized α-Mg regions is reduced. Finally, a full recrystallized grains having distributed small $Mg_{41}Nd_5$ phase is obtained. By XRD analysis two phases are detected namely α-Mg and $Mg_{41}Nd_5$ which are indicated in Fig. 8. Furthermore, EDS analysis to investigate the elemental composition of the phases was performed in both phases. These results are shown in Fig. 9.

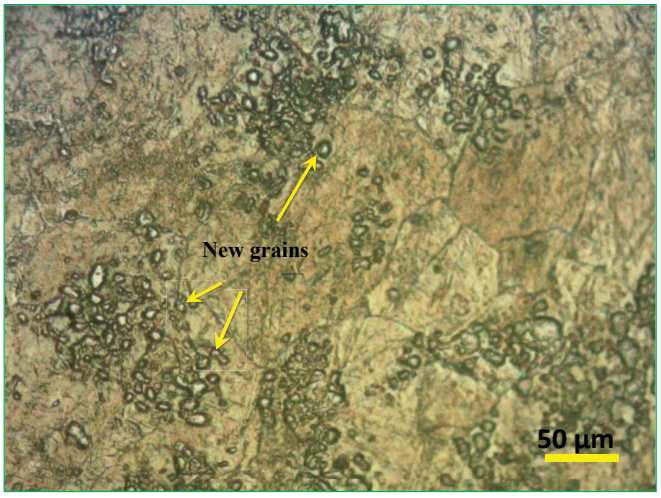

Fig. 6. Nucleation of new grains along the grain boundaries after the first pass of ECAP process

3.3. Microhardness

Microhardness of the samples processed via different conditions is illustrated in Fig. 10a. Each value is the average of at least five tests with 5% scatter error. As shown, Vickers hardness of the samples increases with the increase of the ECAP passes

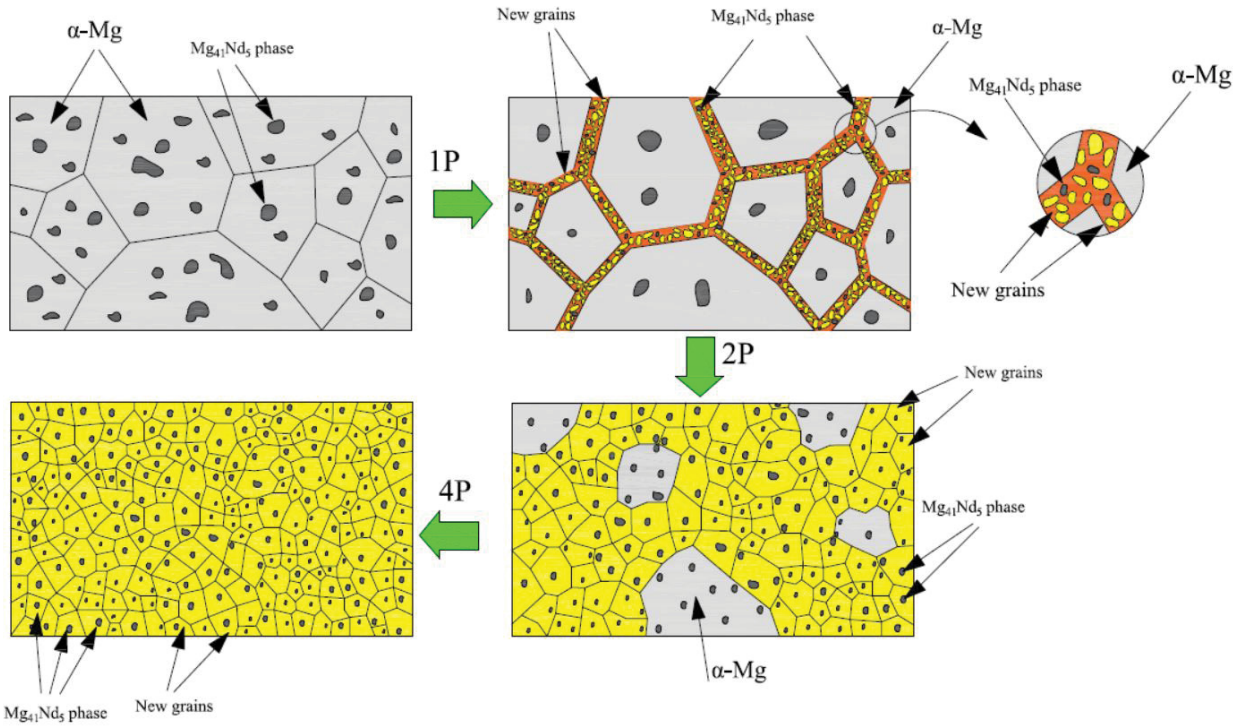

Fig. 7. Schematic of grain refinement process of WE43 in ECAP processing (a) unprocessed sample and after (b) one (c) two and (d) four passes

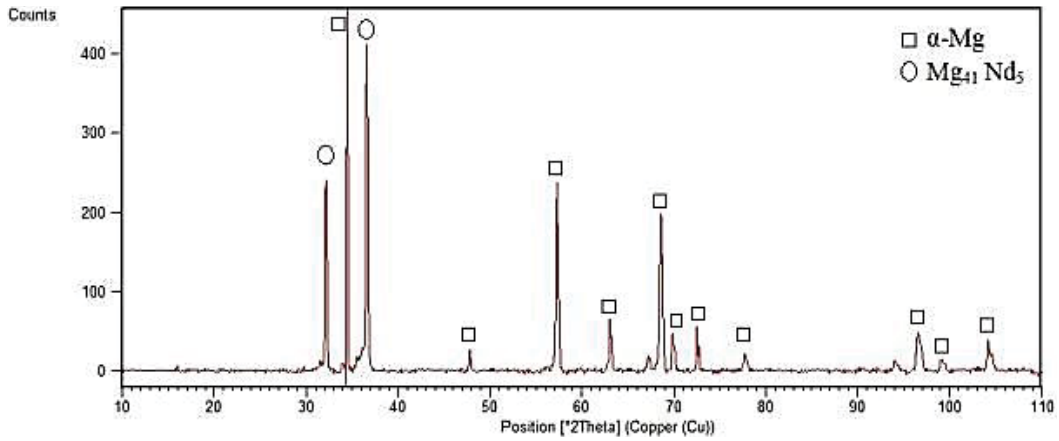

Fig. 8. X-ray diffraction patterns of the unprocessed WE43 alloy

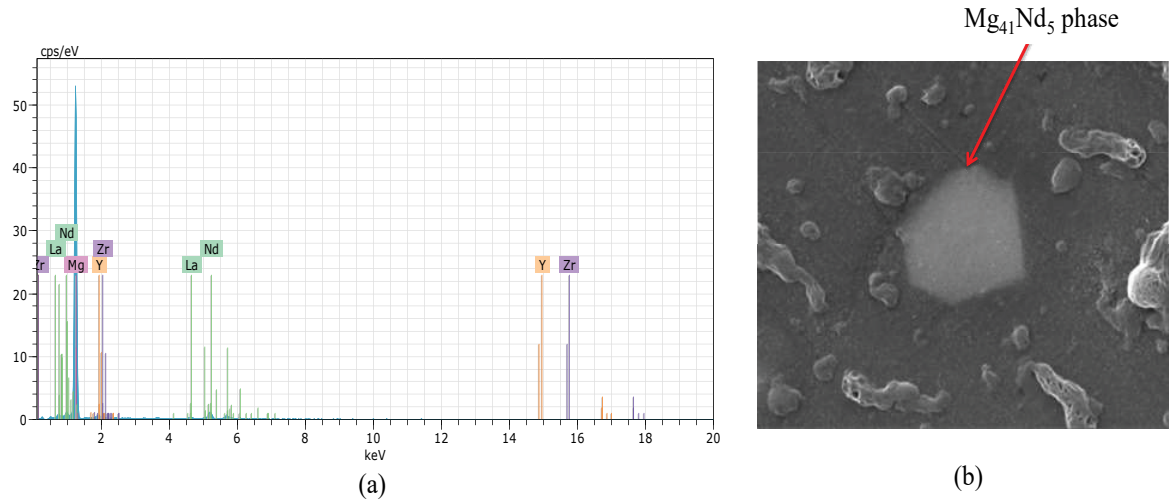

Fig. 9. EDS result of (a) $Mg_{41}Nd_5$ phase and (b) SEM image of $Mg_{41}Nd_5$ phase

due to grain refinement that is in conformance with Hall-Petch relation [21,36]. Not to mention that due to plastic deformation microhardness increases due to the cross-sectional reduction that occurs during the extrusion process. Accumulation of plastic strain enhances the density of defects which are immovable at room temperature. Microhardness test also conducted along the radius of each sample to evaluate microhardness variations in sample cross section. To this end, five points on the sample cross section were considered along A-B path as shown in Fig. 10b. Results show that the maximum microhardness corresponds to a region between the center and the outer diameter of samples. According to Fig. 10b, the center of the samples has the minimum microhardness. However, the as-cast sample has nearly uniform microhardness along its radius. Such difference in microhardness between ECAPed and as-cast samples can be explained by the fact that plastic strain has an effective role in sample microhardness and it is mostly carried on the sample periphery due to higher shear zone at this region [37]. As well, such phenomenon occurs in extruded ECAP samples. As described earlier, an equivalent strain that is applied to each sample is a combination of equivalent strain due to ECAP and extrusion processes. In other words, the strain increases the dislocation density which is one of the key parameters of hardness improvement [38].

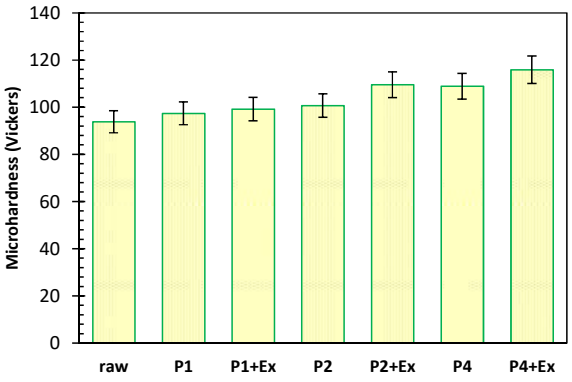

(a)

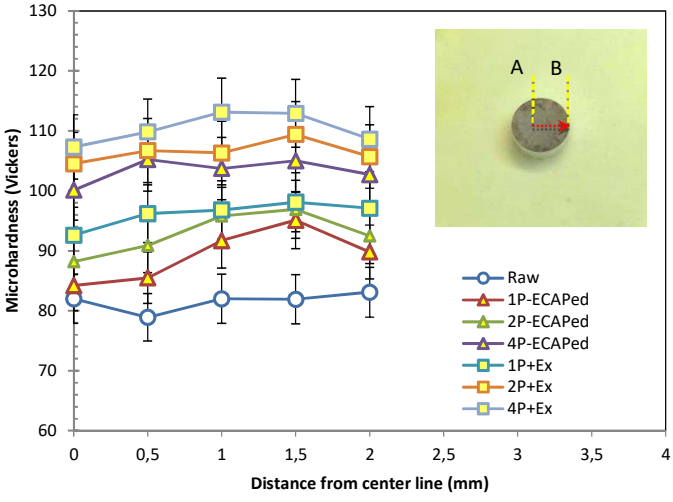

(b)

Fig. 10. (a) Microhardness of samples processed via different conditions (b) Microhardness distribution along the sample's diameter

4. Conclusions

In this study, the effect of subsequent extrusion of ECAPed samples on the mechanical properties and microstructure of WE43 Mg alloy were investigated. The achieved conclusions can be categorized as the following:

- Both of ECAP and extrusion processes enhanced the microhardness of the samples. However, combine extruded samples represented higher microhardness in comparison with the ECAPed samples.
- The homogeneity level enhanced by increasing the number of ECAP passes.
- The maximum microhardness was observed in a region between the center and outer diameter of samples which are processed by ECAP and ECAP + Extrusion.
- Among the ECAPed samples, the highest and lowest strength were obtained in the second and the first pass processed sample, respectively. The four passes processed sample showed the highest elongation to failure with moderate strength.
- The trend in combined multi-pass ECAP and Extruded samples are different with ECAPed specimens.
- The sample processed via first pass ECAP followed by extrusion exhibits an excellent combination of strength and ductility.
- The highest strength was obtained in the sample processed via the second pass ECAP followed by extrusion while the highest elongation was achieved in that processed via fourth pass ECAP followed by extrusion.

Acknowledgements

This work was supported by Iran National Science Foundation (INSF).

REFERENCES

[1] R.Z. Valiev, Y. Estrin, Z. Horita, T.G. Langdon, M.J. Zechetbauer, Y.T. Zhu, Jom. **58**, 33-39 (2006).
[2] M.A. Meyers, A. Mishra, D.J. Benson, Progress in Materials Science **51**, 427-556 (2006).
[3] H. Alihosseini, M.A. Zaeem, K. Dehghani, G. Faraji, Materials Letters **140**, 196-199 (2015).
[4] F. Djavanroodi, M. Ebrahimi, Materials Science and Engineering A **527**, 7593-7599 (2010).
[5] H.S. Kim, Materials Science and Engineering A **315**, 122-128 (2001).
[6] M. Kulczyk, J. Skiba, W. Pachla, Archives of Metallurgy and Materials **59**, 163-166 (2014).
[7] Y. Beygelzimer, V. Varyukhin, S. Synkov, D. Orlov, Materials Science and Engineering A **503**, 14-17 (2009).
[8] Y. Beygelzimer, D. Orlov, V. Varyukhin, Ultrafine Grained Materials **2**, 297-304 (2002).
[9] M. Richert, Q. Liu, N. Hansen, Materials Science and Engineering A **260**, 275-283 (1999).

[10] G. Faraji, M.M. Mashhadi, S.-H. Joo, H.S. Kim, Rev. Adv. Mater. Sci. **31**, 12-18 (2012).
[11] G. Faraji, M.M. Mashhadi, H.S. Kim, Materials Letters **65**, 3009-3012 (2011).
[12] R.Z. Valiev, T.G. Langdon, Progress in Materials Science. **51**, 881-981 (2006).
[13] R.B. Figueiredo, T.G. Langdon, Journal of Materials Science **45**, 4827-4836 (2010).
[14] V.V. Stolyarov, Y.T. Zhu, T.C. Lowe, R.Z. Valiev, Materials Science and Engineering A **303**, 82-89 (2001).
[15] D.-H. Kang, T.-W. Kim, Materials & Design **31**, S54-S60 (2010).
[16] K. Bryła, J. Dutkiewicz, L. Litynska-Dobrzynska, L. Rokhlin, P. Kurtyka, Archives of Metallurgy and Materials **57**, 711-717 (2012).
[17] W. Pachla, A. Mazur, J. Skiba, M. Kulczyk, S. Przybysz, Archives of Metallurgy and Materials **57**, 485-493 (2012).
[18] T. Ying, J.-P. Huang, M.-Y. Zheng, K. Wu, Transactions of Nonferrous Metals Society of China **22**, 1896-1901 (2012).
[19] A. Vinogradov, D. Orlov, Y. Estrin, Scripta Materialia **67**, 209-212 (2012).
[20] W. Kim, Y. Sa, Scripta Materialia **54**, 1391-1395 (2006).
[21] J. Stráská, M. Janeček, J. Čížek, J. Stráský, B. Hadzima, Materials Characterization **94**, 69-79 (2014).
[22] Y. Miyahara, Z. Horita, T.G. Langdon, Materials Science and Engineering A **420**, 240-244 (2006).
[23] G. Garces, M. Muñoz-Morris, D.G. Morris, P. Pérez, P. Adeva, Materials Science and Engineering A **614**, 96-105 (2014).
[24] F. Akbaripanah, F. Fereshteh-Saniee, R. Mahmudi, H. Kim, Materials Science and Engineering A **565**, 308-316 (2013).
[25] P. Minárik, R. Král, J. Pešička, S. Daniš, M. Janeček, Materials Characterization **112**, 1-10 (2016).
[26] P. Minárik, R. Král, J. Pešička, F. Chmelík, Journal of Materials Research and Technology **4**, 75-78 (2015).
[27] F. Witte, Acta Biomaterialia **6**, 1680-1692 (2010).
[28] Y. Iwahashi, J. Wang, Z. Horita, M. Nemoto, T.G. Langdon, Scripta Materialia **35**, 143-146 (1996).
[29] S. Qamar, A. Arif, A. Sheikh, Journal of Materials Processing Technology **155**, 1734-1739 (2004).
[30] X. Zhang, G. Yuan, L. Mao, J. Niu, W. Ding, Materials Letters **66**, 209-211 (2012).
[31] R. Sánchez-Martín, M.T. Pérez-Prado, J. Segurado, J. Bohlen, I. Gutiérrez-Urrutia, J. Llorca, J.M. Molina-Aldareguia, Acta Materialia **71**, 283-292 (2014).
[32] J. Koike, T. Kobayashi, T. Mukai, H. Watanabe, M. Suzuki, K. Maruyama, K. Higashi, Acta materialia **51**, 2055-2065 (2003).
[33] W. Liu, J. Zhang, Z. Zhang, D. Wang, C. Xu, X. Zong, K. Nie, Materials and Manufacturing Processes **32**, 62-68 (2017).
[34] I.-H. Jung, M. Sanjari, J. Kim, S. Yue, Scripta Materialia **102**, 1-6 (2015).
[35] A. Salandari-Rabori, A. Zarei-Hanzaki, S. Fatemi, M. Ghambari, M. Moghaddam, Journal of Alloys and Compounds **693**, 406-413 (2017).
[36] G. Faraji, M.M. Mashhadi, H.S. Kim, Materials and Manufacturing Processes **27**, 267-272 (2012).
[37] T.G. Langdon, Journal of Materials Science **42**, 3388-3397 (2007).
[38] Y. Estrin, L. Toth, A. Molinari, Y. Brechet, Acta Materialia **46**, 5509-5522 (1998).